

# APPLICATION OF MODEL-BASED GEOSTATISTICS FOR NATURAL HAZARDS IDENTIFICATION

H. R. Ghafarian<sup>a</sup>, A. Stein<sup>b</sup>, A. Sharifi<sup>c</sup>

<sup>a,b,c</sup> ITC, Hengelosestraat 99, 7514 AE Enschede, the Netherlands- gafarian15002@alumni.itc.nl

**KEY WORDS:** Model-based geostatistics, Ordinary kriging, Kriging with external drift, Natural hazard.

## ABSTRACT:

Annually much agricultural productions are lost by natural hazards such as flooding, extreme temperature, and drought. In this research we present a procedure to identify such hazards for rice cropping from remote sensing imagery. Extreme temperature is investigated by comparing actual temperatures with tolerance temperatures during the growing stage. Drought is investigated using the evapotranspiration ratio (ETa/ETp) and comparing it with the allowable range. Flooding is studied by finding sudden drops in NDVI values after an extreme rain fall. The procedures are applied to a rice growing area in Iran, 2006. The results, however, did not show any of these hazards to have occurred in the area during the study period. To study spatial effects of hazard, we next created a yield map using model-based geostatistics. We compared ordinary kriging (OK) with external drift kriging (KED). Smaller prediction errors exist when using KED with NDVI and Distance from city as external drift. Cross validation indicates that the straightforward OK that ignores the information from secondary data yields the largest prediction errors (1.36 compare to 0.061 for KED). The results suggest using spatially intensive ancillary data leads to increasing the accuracy of prediction of yield map.

## 1. INTRODUCTION

Agricultural productions as a main part of the food provider have a strategic role in the world. Annually much is lost, however, due to natural hazards such as extreme temperature, flooding and drought. Identification of the effects of each of those can help to control and protect and be a support for farmer and the manager. Such identification may be better possible nowadays with increasing availability of continuous weather data, remote sensing imagery and modern yield mapping methods.

Each natural hazard has a different impact on rice. Temperature affects rice growth during the whole growing stage as well as in the final production. Rice is sensitive to high-temperature stress at almost all the stages of its growth and development (Tashiro, 1991). These effects are also shown in rice yield predictor models using the more effective parameter in growing stage of rice. In the temperature range occurring in Iran, these models generally show that an increase in temperature decreases the final yield of rice (Amien, 1999 ; Karim, 1996). Agricultural drought (Wilhite, 1987) links drought to agricultural impacts, focusing on precipitation shortage, differences between actual and potential evapotranspiration, soil water deficit and reduced ground water or reservoir levels, and so forth. Several indices are capable for investigating drought in a region. Examples are the Vegetation temperature condition index (CTCI) and the Water deficit index (WDI) Both can be observed with remotely sensed imageries and have been used in the past to identify drought stress at the regional scale (Ranjan Parida, 2006). The problem of flood in rice fields is depth and duration accumulation of water after heavy rainfall (Suwat, 1996) and subsequent field run off. Dynamic models are regularly used for flood detection (Alkema, 2003; Rasamee, 1992). These models require river inflow and outflow data, meteorological data and DEM maps are necessary. Often, these models are based upon water balances.

The objective of this research was to develop a procedure of identifying the impacts of natural hazards, e.g., extreme temperature, drought and flood on rice yield in time and space. For each hazard, we define an indicator, being a variable with a threshold. For hazards in time, we used time series graphs showing variation of the indicators. Exceedance of thresholds shows us the presence of a hazard in time during the growing stage. Hazards in space are addressed using the rice yield map. They relate to patterns in particular with low yield values. We used model-based geostatistics for this purpose and compared ordinary kriging and kriging with external drift to find the better model for rice yield creation. The study was performed in the Some'e-sara Township located in Iran.

### 1.1 The study area

This research has been conducted in Some'e-sara in the west of Gilan Province in Iran. The county of Some'e-sara is situated on the Northern part of Iran between 37.25<sup>0</sup>N to 37.50<sup>0</sup>N and 49.04<sup>0</sup>E to 49.55<sup>0</sup>E.

### 1.2 Description of available data

The data used in this study were obtained from three sources, time series raster maps (NDVI, Biomass, Evapotranspiration actual, Evapotranspiration potential, soil moisture and Evapotranspiration deficit) as derived from the MODIS imagery (Sharifi, 2006), 140 days meteorological data was obtained from six meteorological Stations and actual yield measured from 224 farms.

### 1.3 Data processing

The aim of data processing was extract value of each available data for each farm. Geostatistical interpolation was used to create 140 daily maps from meteorological data (Temperature and Rainfall). Then a big database containing time series value of each variable for each farm was formed.

## 2. METHODOLOGY

### 2.1 Identification of natural hazards in time

Identification of natural hazards needs monitoring their related indicator in time and finding the pattern of them in the space. For investigation each hazard in time, a graph was plotted showing the variation of its indicator and related threshold versus time. In this section the concept of each method and the way to find each indicator is summarized.

### 2.2 Determination of indicator and threshold for each hazard

Indicator for each of the three hazards was determined as follow: Temperature as a function of time  $T(t)$  was compared to both the lowest and the highest favorite temperatures ( $T_{1,low}(t)$  and  $T_{1,high}(t)$ , respectively) and the the lowest and the highest tolerance temperatures ( $T_{2,low}(t)$  and  $T_{2,high}(t)$ , respectively) for rice growing in the costal part of Iran for each variety. The temperature in different growing stage of rice has been measured in Gilan meteorological organization located in Rasht province (Gilan meteorological station, 2003), Table 1.

Phenological stage	Min Favorite (°c)	Max Favorite (°c)	Min Tolerance (°c)	Max Tolerance (°c)
Germination	15	20-25	10	30
seeding	20	25-29	12	30
Tillering	20	25-29	12	30
Stem Elongation	20	27-29	14	34
Flowering	22	27-32	17	35
Milk Grain	23	27-32	17	35
Dough Grain	23	27-32	17	35
Mature Grain	22	25-30	17	33
Harvesting	22	25-30	15	33

Table 1. Favorite and tolerance temperature (max and min) for different phenological stage of rice in coastal part of Iran (www.Guilanmet.ir)

For drought identification, we selected the relative evapotranspiration ( $ETr(t) \in [0,1]$ ), being the ratio of the actual ( $ET_{ac}(t)$ ) and the potential ( $ET_{pot}(t)$ ) evapotranspiration of the crop at moment t. It expresses the degree to which a certain land can suit the water demand of a plant as a consequence of drought occurrence of the different levels of the water scarcity (Petrasovits, 1990), Table 2.

ETr range	Explanation
1.0 - 0.8	water scarcity of the plant is only theoretical, because the water supply to the plants is continuous and not limited
0.8-0.5	The water demand is still continuous, but it is getting increasingly restricted
0.5-0.3	Water scarcity is high, the water supply to the plants is periodical and restricting, therefore water-stress develops
< 0.3	Strong water stress occurs, causing considerable biomass and yield deficiency, and when this stage lasts long also the death of the plant.

Table 2. Relative evapotranspiration classification (www.iwmi.cgiar.org)

Floods, i.e. occurrence of excessive water logging, may occur after an extreme rainfall event. Rainfall, however, can be highly localized, causing flooding in one area but not in another area. It depends on parameters like rainfall intensity, soil infiltration rate, soil texture, ground slope and proximity of a river or channel. We used the NDVI value as an indicator at the farm site. This indicator suddenly drops if a flood damages the rice by rushing off some of the crop. The NDVI graph was compared with rainfall data.

### 2.3 Identification of natural hazards in space

To investigate spatial patterns in rice yield with possible hazardous causes, we created a yield map using model-based geostatistics. Geostatistics, based on the theory of regionalized variable (Goovaerts, 1977) is optimal for interpolation of spatial data, allowing incorporation of spatial dependence between observations. Here we consider model-based geostatistics (Diggle, 1998). It has been shown (Tabios, 1985; Goovaerts, 2000) that geostatistical methods like kriging are superior to other methods for estimating spatial data in unvisited locations (Kriging, 1951). In this study we used ordinary kriging (OK) and kriging with external drift (KED) (Isaaks, 1989; Wackernagel, 1998). The difference of KED is that secondary data that are more densely available can be used as auxiliary data for prediction of a target variable (Wackernagel, 1998; Goovaerts, 1999; Hengl, 2003).

### 2.4 Ordinary kriging (OK) and external drift kriging (KED)

Ordinary kriging serves to estimate a value at a point of a region using the variogram. The value  $Z(x_0)$  at the unsampled location  $x_0$  is estimated as a weighted average of sample values  $Z(x_a)$  at locations  $x_a$  around it. We thus consider predictors that are linear in the observations, i.e. each observation is assigned a weight, which is without bias. The optimal predictor is denoted with  $\hat{Z}(x_0)$ . It is linear in the observations, therefore

$$\hat{Z}(x_0) = \sum_{i=1}^n w_i Z(x_i) \tag{1}$$

with as yet unknown weight  $w_i$ . The prediction error  $\hat{Z}(x_0) - Z(x_0)$  is assumed to have expectation equal to zero and that it has the lowest variance among all linear unbiased predictors:  $Var(\hat{Z}(x_0) - Z(x_0))$  is minimal.

Variogram values between the observation are summarized in the  $n \times n$  matrix  $G$ , i.e, the elements of  $(G)_{ij} = g(|x_i - x_j|)$ . Notice that  $g_{ij} = g_{ji}$  and that the diagonal elements  $g_{ii}$  of  $G$  are equal to 0. Variogram values between the observation locations and the prediction location are contained in the vector  $g_0$ . The unbiased predictor with lowest variance of the prediction error, linear in the observations is given by:

$$\hat{Z}(x_0) = \sum_{i=1}^n w_i Z(x_i) = \hat{\mu} + g_0' G^{-1} (Z - \hat{\mu} \cdot X) \tag{2}$$

where  $X$  is the design matrix. In the case of OK,  $X$  consists of one vector with values 1 only, whereas for KED is has two columns, the first consisting of the values 1, the second of the values of the external drift. The vector  $Z$  is he vector of the observable in the observation locations. An estimate for the value of the trend parameters  $\hat{\mu}$  are found by means of the generalized least squares estimator

$$\hat{\mu} = (XG^{-1}X)^{-1} XG^{-1}Z \tag{3}$$

Weights depend on the degree of correlations among sample points and estimated point. The sum of weights is equal to 1 (this is specific to ordinary kriging):

$$\sum_{\alpha=1}^n w_{\alpha} = 1 \tag{4}$$

Thus ensuring no bias. All calculations were carried out with the package geoR.

### 3. RESULT AND DISCUSSION

#### 3.1 Identification of extreme temperature

The hazard due to extreme temperature causing yield losses was investigated by comparing the actual temperature with low and high tolerance temperature. To find the effect of temperature on rice yield losses, at the first we should investigate it in the farm with lowest yield and compare the fluctuation of temperature in this farm with highest yield farm. To do so, we considered 4 selected farms: the two with the highest yields and the two with the lowest yields. Fluctuation of daily max and min temperature for whole growing stage of these four points has been showed in the Figure 1.

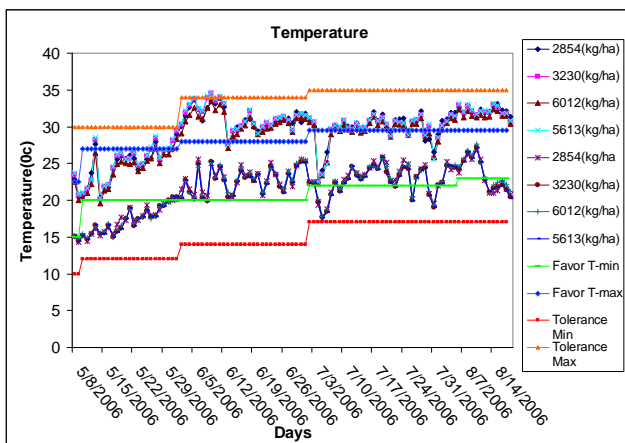


Figure 1. Temperature fluctuations for four points in whole growing stage

This graph shows the maximum and minimum temperature changes in the four farms. The low and high yield farms have 2854, 3230, 5613 and 6012 (kg/ha) actual yield respectively. The value of favour and tolerance temperature was obtained from Table 1. We notice first that the recorded temperatures are similar, which is caused by the uniform temperature in the area, and the fact that there were only 6 meteorological stations. The result shows that none of these points exceed from two tolerances for max and min temperature and it means, therefore, that no extreme temperature hazard occurred in 2006 in the study area.

#### 3.2 Identification of drought

To find drought hazard in this study area, we plotted relative evapotranspiration values against time and compared those values to allowable value based on Table 2 (see Figure 2). These values have been taken from 13 MODIS derived raster maps; the horizontal axis is the time interval between different images. For this part also we selected the same four points in previous part. This graph shows all the

point stands between allowable rang. So we conclude that there also was no drought hazard in 2006.

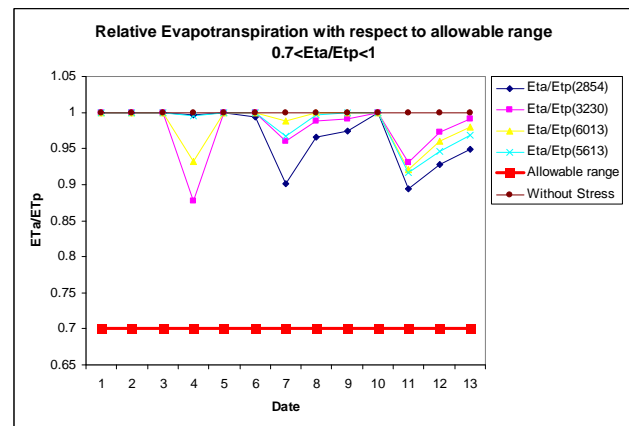


Figure 2. Relative Evapotranspiration value against time

#### 3.3 Identification of flood

The indicator for flood detection in study area was NDVI value. The normal NDVI value for whole growing stage of rice has been showed in Table 3.

Rice growing stage	Rice age (day)	NDVI value
Planting	30 days before transplanting stage	0.253-0.365
Transplanting	20	0.397-0.483
Growing	45	0.720-0.811
Reproducing	45	0.611-0.711
Harvesting	After 120 days	0.536-0.603

Table 3. NDVI of rice growth stage.

The rainfall and NDVI graph from starting point up to harvesting stage have been shown in Figure 3 and Figure 4. We have just one day with heavy rainfall that shown in Figure 3. If this rainfall had caused flood, a sudden drop in NDVI value should be seen some day after it. But graph 4 doesn't show this change. So we get a good result that we don't have any flood in this season that cause damage to paddy field. The first stage for starting work is creating a geodata base. It consists of coordinate of each farm point (x, y), values of actual yield for each farm point and also 13, 13 and 13 values for NDVI, ET-deficit and biomass as co-varible respectively. The number of my farm in this research was 224 from two different varieties (166 point for one variety and the rest for another). Because the number of point and spatial dispersal of them must be adequate, we selected the first one (166 farm points).

At the first glance, Plotting the data value versus coordinates may help us to find the existence of some trends visually (Figure 5 top right and bottom left plot). The different signature in the top left plot shows different class of data based on its value. Some point that is near to each other has different signature and it means we have high different value in small distance and it is the evidence of existence nugget effect in our data. The histogram of data value shows that our data has normal distribution (Figure 5 bottom right plot).

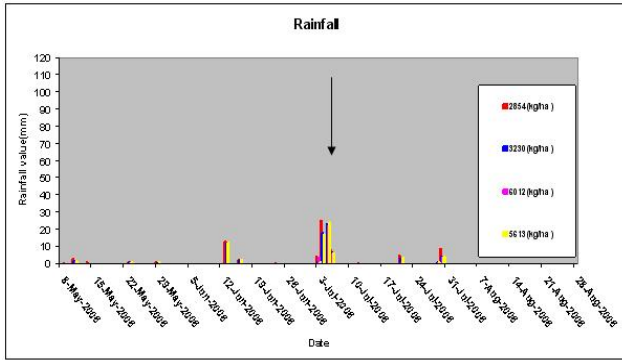


Figure 3. Rainfall value for whole growing stage of rice in study area

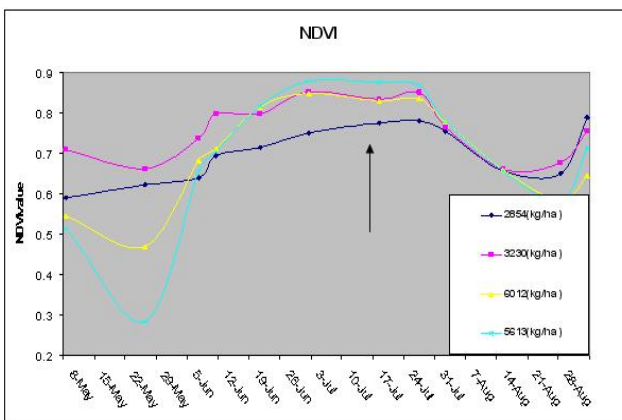


Figure 4. NDVI value for whole growing stage of rice in study area

The experimental variogram of yield data computed from the 166 farm points calculated. Because of existence any anisotropy in data only omnidirectional variogram was computed. After plotting the experimental variogram we fit some models to find initial value for further analysis. We first fitted a variogram model by eye. This procedure allows the experimenter to take into account his expertise as well as additional information about the data. Table 5 shows the values for sill, range and nugget, for a spherical model.

Next we used restricted maximum likelihood (RML) and weighted least squares (WLS). The initial values for these computations are those in Table 5, the results of implementation are shown in Table 6 and Figure 5 respectively.

### 3.4 Accuracy assessment of fitted model

In order to find the best model between WLS and RML we must calculate the residual (different between each bin value to estimated one by model using following Equation 5).

$$Residual = \frac{\sum_{i=1}^{10} (\gamma(d_i) - \gamma_m(d_i))^2 * N(p)_i}{\sum_{i=1}^{10} N(p)_i} \tag{5}$$

$\gamma(d_i)$  = variogram value of the  $i$ th bin

$\gamma_m(d_i)$  = Estimated value from model

$N(p)_i$  = Number of pairs of points for the  $i$ th bin

The residual calculation shows that this value for RML model is  $2.39E+09$  and for WLS are  $8.88E+08$ . So because the residual for WLS is lower than RML model, we selected the WLS model as nugget effect estimation model.

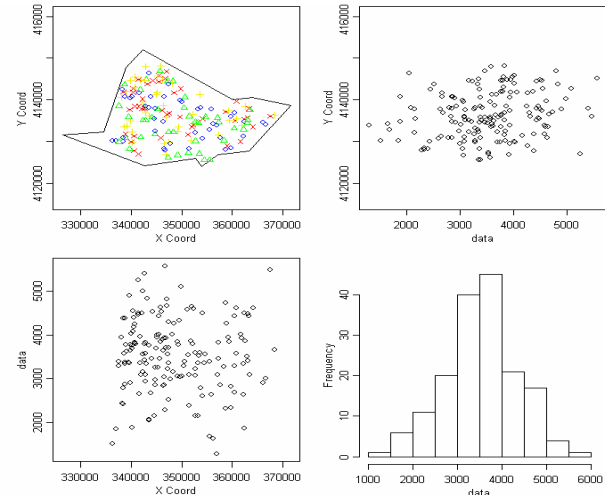


Figure 5: plot data value against coordinate and histogram of data

Covariance model	sigmasq( $C_1$ )	phi(range)	tausq(nugget)
spherical	252000	1670	407000

Table 5: Initial value of theoretical model captured by eye fitting

Used model	Covariance model	Sigmasq ( $C_1$ )	Phi (range)	Tausq (nugget)
RML	spherical	382416	2225	309636
WLS	spherical	246280	1551	406553

Table 6: Model parameters estimated by RML and WLS

### 3.5 Map production using ordinary kriging

Figure 6 shows the yield (a) and standard deviation (b) map based on the parameter estimated by WLS. The result shows that only in farm points we have lower standard deviation. Because the ordinary kriging used the mean of neighbours of each point for prediction, the final point shows that only the value near to each farm point has lower standard deviation.

The result shows that dispersal of low yield farms in the study area are more or less equal and we cannot see any trend in the study area. Also near to these low yield farms we have some farm with high yield. So if we had hazards in this study area, we would see the effect of them in separated area.

### 3.6 Creating yield map using co-variable data

Co-variable data must have a correlation with target value. In order to find co-variable at the first time as a previous knowledge we selected time series NVDI (n1... n18), ET-

deficit (e1... e13), biomass (b1... b13) and distance (dis) to the main city (some'e-sara).The NDVI can assess whether the target being observed contains live green vegetation or not. So this value can say about the health and the situation of plant in the growing stage. Biomass value computed from MODIS imagery and SEBAL model that take in to account temperature, vapour pressure, radiance and other meteorological parameter. So this parameter can show the process of growth in a plant. ET-deficit value can show the situation of water adequacy in plant canopy. Distance to city may help to identify the accessibility of farm and managerial problem due to far distance to city on final yield. To select which of this value is more relevant to yield we used step wise regression.

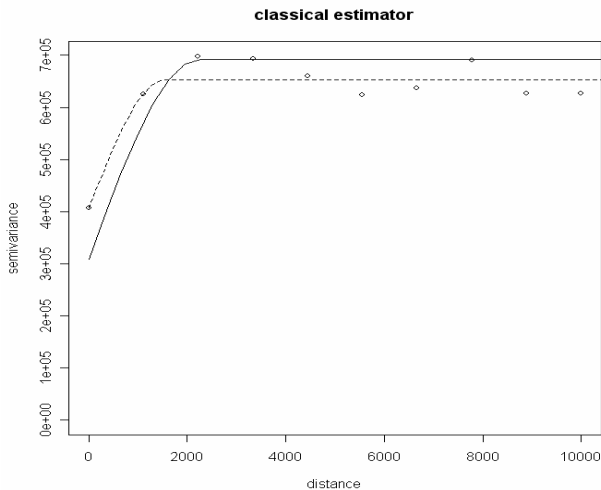


Figure 6: Fitting theoretical variogram using RML and WLS

Except for a high correlation between yield and n5 (r =0.21), only low or moderate correlations (r =0.009 to r =0.207) were observed among yield, NDVI, ET-deficit and Biomass. But the final result of stepwise regression select n5 and dis to city as more correlated co-variables (Table 7).

The linear regression results between thesis variable and yield have been mentioned in Table 8. This table shows all the combination between yield value and co-variable is significant and we selected all possible co-variables in order to find the best model that can produce more precise one for yield map production. The higher multiple R<sup>2</sup> (0.08142) is for NDVI+DISTANCE and lower one (0.02808) for DISTANCE. The final result of using these co-variables has been shown in Figure 6. Because of using all co-variable and target data to calculation of mean in moving window, the results of using co-variables data cover the whole study area. The comparison between ordinary kriging (OK) and kriging with external drift inferred that KED can produce more precise map than ordinary kriging.

Pearson correlation	Yield	Sig.(1-tailed)	Yield
n5	0.211	n5	0.003
dis	0.168	dis	0.015

Table 7: Correlation coefficient and significant parameter for whole data

### 3.7 Comparison between ordinary kriging and kriging with external drift

In order to assess the better model for yield map creation we used the cross validation method (Isaaks,1989). In cross-validation, a portion of the data is set aside as training data leaving the remainder as testing data. The quality of performance of the model on the testing data reflects how well it would perform. In the Table 9 the final result achieved by cross validation will be shown.

Variable	Multiple R <sup>2</sup>	Parameter	Estimate value	Std. Error	t value	Pr (> t )
NDVI	0.04464	intercept	2090.0	527.7	3.961	<0.00011 ***
		slope	1926.2	695.8	2.768	0.006282 **
DISTANCE	0.02808	intercept	3.205e+03	1.664e+02	19.261	< 2e-16 ***
		slope	3.020e-02	1.387e-02	2.177	0.0309 *
NDVI+DISTANCE	0.08142	intercept	1.560e+03	5.589e+02	2.791	0.00588 **
		ndvi	2.118e+03	6.885e+02	3.077	0.00246 **
		dis	.477e-02	1.361e-02	2.555	0.01154 *

Table 8: Linear regression between co-variable and target value (yield)

Models Implemented	OK without drift		KED_NDVI		KED_Distance		KED_NDVI Distance	
	errors	Std .error	errors	Std .error	errors	Std .error	errors	Std .error
Minimized weighted sum of squares	5.10E+12		2.18E+12		5.99E+12		2.78E+12	
Min	-2087	-2.6	-1986	-2.5	-2016	-2.5	-1892	-2.4
1 st Qu.	-470.6	-0.58	-484.3	-0.6	-409.8	-0.51	-513.6	-0.7
Median	12.75	0.016	16.51	0.02	-0.9	-0.001	4.024	0
Mean	-1.36	-0	-0.41	-0	-0.83	-6E-04	-0.061	0
3rd Qu.	489.3	0.6	536	0.68	551.3	0.68	563.2	0.7
Max	2011	2.604	2342	2.89	1950	2.593	2475	3.1
std	804.26	1.01	809.7	1.03	799.51	0.99	802.72	1

Table 9: Cross validation result for different model implemented.

## 4. CONCLUSION AND RECOMMENDATION

This research addresses the need of analyzing and studying the extreme temperature, drought and flood using temporal MODIS derived maps which were available for this study and meteorological data in 224 rice farms in some'e-sara located in north of Iran in 2006. The final result of this study shows that the natural hazards didn't occurred in this area in 2006.

Dealing with a large volume of meteorological dataset for a time-series of 140 days, huge number of time series raster maps such as NDVI, Biomass, ET actual (Evapotranspiration) and ET potential derived from MODIS imagery by the previous work done at Iran (Sharifi,2006) and investigated three different hazards (Exterem temperature, Flood and Drought) in time and

space make the study not only complicated but make it difficult to analyze.

Table 9 shows that the KED method with different external drift has lower bias than Ok without external drift. It means that the mean average error (MAE) is near to zero. The mean error of ordinary kriging without external drift is -1.36 and for kriging with NDVI+Distance as external drifts is -0.061, so the best unbiased method is KED with NDVI+Distance as external drift.

To identify the hazards, we need to investigate them in space and time. To recognize the natural hazards in time, we created time series graphs showing the variation of related indicator for each hazard and compared them to allowable rang. To investigate spatial pattern in rice yield with possible hazardous causes, we created a precise yield map using Model-based geostatistics.

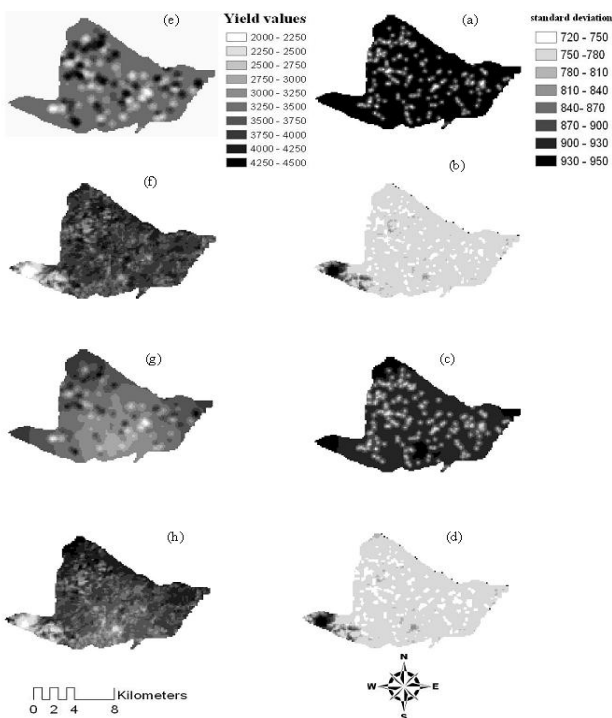


Figure 6: a,b,c,d Predicted yield map using OK, KED with NDVI, Dis and NDVI-Dis as external drift respectively. E,f,g,h Standard deviation maps for OK, KED with NDVI, Dis and NDVI-Dis as external drift respectively.

To find the extreme temperature hazard I compared the fluctuation of daily actual temperature with threshold of temperature for rice. The result showed extreme temperature hazard didn't have any effect in the study area in 2006 (see Figure 1).

For finding drought hazard I calculated the evapotranspiration ratio (ETa/ETp) for the whole time of growing stage of rice and compared it with allowable range. The result showed that evapotranspiration ratio values did not exceed from allowable range and therefore drought wasn't occurred in this area in 2006 (see Figure 2).

Flood was investigated by finding any sudden drop in NDVI value after extreme rainfall in the study area in 2006. The result showed that we had only one extreme rainfall in the growing

stage of rice in the study area and sudden drop in NDVI value wasn't seen (see Figure 3, 4).

Geostatistical methods that utilized spatially correlated secondary information increased the quality of maps of rice yield as compared to OK. Although the yield values were very gentle over the study area, a significant linear relation exists between the yield as a target and NDVI and distance to city as co-variable value. As NDVI and Distance to city were exhaustively known, it was used for mapping the rice yield over the study area. Ordinary kriging and Kriging with external drift (KED) were used.

The results showed that KED provides better prediction on average than OK. This is because the KED integrates not only the exhaustive information on NDVI and Distance into the prediction equations but also the spatial correlation between the rice yield and the NDVI and Distance to city.

There are several reasons why we could not detect disasters. First, it could be the case that disasters were absent during this year, although oral reports provided a clear indication of their presence. Secondly, in particular the meteorological data were samples rather coarsely. Rainfall events can be very much local, requiring very detailed rainfall information, and that information was apparently missing. Thirdly, there could have been other factors leading to very low yield values at some farms. Typical examples would be the quality of the management, availability of technological means, availability of manure and herbicides, poor soil conditions and other circumstances that could not be collected using remote sensing imagery. We hope to be able to continue this work in the near future. To our impression, the study shows the interest of using a combination of outlier diagnostics in combination multivariate model-based geostatistics tools in mapping rice yield.

## REFERENCE

Tashiro, T., and Wardlaw, I. F., 1991. The Effect of High Temperature on the Accumulation of Dry Matter, Carbon and Nitrogen in the Kernel of Rice. *Functional Plant Biology*, **18**(3): p. 259-265.

Amien, I., Redjekiningrum, P., Kartiwa, B. and Estiningtyas, W., 1999. Simulated rice yields as affected by interannual climate variability and possible climate change in Java. *climate change*, **12**: p. 145-152.

Karim, Z., Hussain, S.G., and Ahmed, M., 1996. Assessing impacts of climate variations on foodgrain production in Bangladesh. Kluwer Academic Publishers, Dordrecht, Netherlands, p. 53-62.

Wilhite, D., and Glantz, M.R., 1987. *Understanding the drought phenomenon*. Boulder, Colo., Westview Press, p. 11-27.

Ranjan Parida, B., 2006. Analysing the effect of severity and duration of agricultural drought on crop performance using Terra - MODIS satellite data and meteorological data. ITC: Enschede. p. 92.

Suwat, I., 1996. *Study on rice yield due to flooding*. kasetsart university, Bangkok.

Alkema, D., 2003. Flood risk assessment for EIA : environmental impact assessment, an example of a motorway

- near Trento, Italy. In: Studi Trentini di Scienze Naturali : Acta Geologica, 78(2003), pp. 147-154.
- Rasamee, S., 1992. Flood forecasting using a hydrologic model and GIS : a case study in Huai Nam Chun catchment, Pa Sak watershed, Phetchabun, Thailand. ITC: Enschede. p. 150.
- Sharifi, A., 2006. System Description for Rice Damage Assessment, Caused by Natural Hazards, Using Remote sensing technology and bio-physical models (on going project). International Institute for Geo-Information Science and Earth Observation (ITC).
- Gilan meteorological station, 2003. R. Determination of meteorological parameter effect on different phenological stage of rice in coastal part of iran. www.guilanmet.ir.
- Petrassovits, I. 1990. *General Review on Drought Strategies*. in *In Transactions of the 14th Congress on Irrigation and Drainage*. Rio de Janeiro: International Commission on Irrigation and Drainage(ICID).
- Diggle, P.J., Tawn, J.A. and Moyeed, R. A., 1998. *Model based geostatistics (with discussion)*. Applied Statistics. **47**: p. 299-350.
- Goovaerts, P., 1977. *Geostatistics for natural resources evaluation*. Oxford Univ. Press, New York. 483.
- Tabios, G.Q., and Salas, J.D., A ,1985. comparative analysis of techniques for spatial interpolation of precipitation. Water Resources Bulletin. **21**: p. 365-380.
- Goovaerts, P., 2000. Geostatistical approaches for incorporating elevation into the spatial interpolation of rainfall. Journal of Hydrology. **228**(1-2): p. 113-129.
- Krige, D.G., A, 1951. *statistical approach to some basic mine valuation problems on the Witwatersrand*. J. of the Chem., Metal. and Mining Soc. of South Africa. **52**: p. 119-139.
- Wackernagel, H., 1998. Multivariate geostatistics: an introduction with application, ed. n. Edition. Springer-Verlag.
- Goovaerts, P., 1999. Using elevation to aid the geostatistical mapping of rainfall erosivity. CATENA, **34**(3-4): p. 227-242.
- Hengl, T., Geuvelink, G.B.M., and Stein, A., 2003. *Comparison of kriging with external drift and regression-Kriging* Technical note, ITC, Available on-line at [http://www.itc.nl/library/Academic\\_output/](http://www.itc.nl/library/Academic_output/).
- Isaaks, E.H., and Srivastava, R.M., 1989. *An Introduction to Applied Geostatistics*. Oxford Univ. Press, New York, Oxford.
- Ribeiro Jr., P.J.D., P.J., 2001. *geoR: A package for geostatistical analysis*. R-NEWS, **1**: p. 15-18.
- Wackernagel, H., 1998. Multivariate geostatistics: an introduction with application, ed. n. Edition. Springer-Verlag.

